

Cooperative Ordering at Liquid Crystal Interfaces and Its Role in Orientational Memory

Douglas M. Scott,[†] Nickolaus A. Smith,[‡] Joseph J. Valente,[§] Rachel Adams,[†] Kevin Bufkin,[†] and David L. Patrick^{*,†}

Department of Chemistry, Western Washington University, 516 High St., Bellingham, Washington 98225; Chemistry Division, Los Alamos National Laboratory, Los Alamos, New Mexico 87545; and Novartis Pharmaceuticals Corporation, One Health Plaza, East Hanover, New Jersey 07936

Received: September 24, 2009; Revised Manuscript Received: November 12, 2009

Orientational memory in interfacial liquid crystal films occurs when cells heated above the isotropic transition temperature return to their initial ordered texture upon cooling. First observed over 80 years ago, the origins of orientational memory, which is sometimes called the surface memory effect, remain poorly understood. In this study, films of the thermotropic liquid crystal 4'-octyl-4-cyanobiphenyl on graphite were studied by scanning tunneling and polarizing optical microscopy. Strong orientational memory was observed despite relatively weak molecule–surface interactions of the kind previously thought to be responsible for this effect. By preparing cells in a uniformly oriented initial reference state and separately measuring bulk and surface order parameters as systems were thermally disordered, cooperative interactions were found to play an important role, leading to the recovery of long-range order that neither the bulk nor surface layers alone retained. When the surface and bulk layers were partially decoupled using a magnetic field, orientational memory in the surface layer almost disappeared. The findings provide a new interpretation of the origins of orientational memory in liquid crystal films and underscore the potentially important role of cooperativity in bulk ↔ interfacial liquid crystal interactions.

When a liquid crystal (LC) contacts a solid surface, a single molecular layer at the interface can dictate the director orientation throughout the entirety of the bulk fluid.^{1,2} Likewise, when a molecular layer of LC adsorbs to a surface, its orientation is affected by the supernatant fluid.³ Interactions between LCs and surfaces which bound them are therefore bidirectional. Because the surface properties of LCs are very different from those of the bulk,⁴ the bidirectional nature of these interactions raises interesting possibilities for emergent cooperative phenomena, leading to behavior that neither the interfacial nor bulk phases alone would display. Although cooperativity is an essential feature of bulk LCs as well as many other chemical, physical, and biological systems, its role in the surface properties of LCs is largely unexplored.⁵ Since bulk ↔ interfacial layer interactions occur whenever a LC contacts a surface however, it has the potential to influence a variety of interfacial LC phenomena, ranging from alignment to wetting.

One case where cooperativity may be particularly important is in the so-called surface memory effect (SME), which occurs when the LC layer adsorbed to a solid substrate undergoes disordering at a higher temperature than the bulk LC. This leads to the appearance of “memory” wherein an entire LC cell can repeatedly return to its initial orientational state after being temporarily heated above the bulk isotropic transition temperature, T_{NI} .^{6,7} In some cases the SME can be remarkably strong, persisting in cells heated more than 50 °C above T_{NI} for many minutes or hours.^{8–10} The origins of such strong memory have puzzled researchers for over 80 years, and much effort has been devoted in an attempt to explain it.^{6–13} The first modern

interpretation was proposed by Clark, who suggested based on observations of the SME on polyimide that LC-induced partial alignment of polymer chains might be responsible.⁷ Other proposed mechanisms have included displacive adsorption-driven disordering,⁸ electrical double layer effects,¹¹ and the existence of a surface layer with high rotational viscosity.¹² The most widely cited theory, due to Ouchi et al.,¹³ is that LC molecules adsorbed at the surface become orientationally trapped in deep potential wells, and these molecules alone re-establish order throughout the cell upon cooling below T_{NI} . Heating results in gradual loss of memory as trapped molecules undergo thermally activated rotational diffusion.

In this work, the SME was studied in LC films on highly oriented pyrolytic graphite (HOPG), where LC molecules interacted with the surface through relatively weak van der Waals forces and there were few defect sites for strong trapping. Consequently, each time the cell temperature was cycled across T_{NI} , both the bulk and surface directors were free to adopt new orientations, with the resulting alignment caused by cooperative interactions coupling the two layers. By preparing cells in a uniformly oriented initial reference state and combining optical and scanning tunneling microscopy (STM) to separately measure bulk and surface order parameters as systems were thermally disordered, we found that cooperativity plays a dominant role in memory, leading to the emergence of long-range order that neither the bulk nor surface layers alone displayed. When the surface and bulk layers were decoupled using a magnetic field, orientational memory in the surface layer almost disappeared.

The LC used in this study, 4'-octyl-4-cyanobiphenyl (8CB, $T_{\text{cryst-SmA}} = 21.5$ °C, $T_{\text{SmA-N}} = 33.5$ °C, $T_{\text{NI}} = 40.5$ °C), forms a single, polycrystalline monolayer on graphite at room temperature (inset, Figure 1). Molecules adsorb with their long axis in the plane of the substrate, and anchoring is planar, with the easy axis approximately parallel to the long axis of molecules

* To whom correspondence should be addressed. E-mail: patrick@chem.wvu.edu. Tel: 360-650-3128. Fax: 360-650-2826.

[†] Western Washington University.

[‡] Los Alamos National Laboratory.

[§] Novartis Pharmaceuticals Corporation.

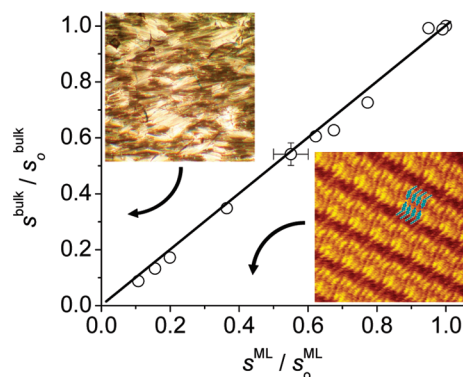


Figure 1. Orientational order in the bulk LC and the monolayer adsorbed to graphite were tightly coupled. Data are from thin cells for a range of heating temperatures and times. The line has a slope of 1.0 and passes through the origin. Insets show a representative 1×1 mm optical micrograph and 20×20 nm STM image. The STM image shows a left-handed domain with model overlay of molecules in one unit cell [constant height image, $I = 1.0$ nA, $V = -0.4$ V, 80/20 Pt/Rh tip].

on the surface. The monolayer crystallizes at a temperature of $T_c = 26\text{--}28^\circ\text{C}$,¹⁴ and melts at $T_m = 33.5 \pm 1^\circ\text{C}$.¹⁵ The melting transition coincides with loss of crystalline order, as determined by in situ STM observation of heated films,¹⁵ although it is probable that a partially ordered surface phase continues to exist up to higher temperatures.¹⁶

Samples were prepared by placing a droplet of 8CB on HOPG and covering with a clean glass coverslip, forming cells $20\text{--}40\ \mu\text{m}$ thick. For a few experiments noted in the following, very thick cells ($2000\text{--}3000\ \mu\text{m}$) were used, constructed by submerging the substrate in a trough filled with 8CB and covering with a coverslip. Cells were placed in a 1.2 T electromagnet oriented with the field axis in the substrate plane, heated to 100°C for 2 min., and gradually cooled to room temperature. This procedure, which has been called “liquid crystal imprinting”,³ results in uniformly aligned cells (orienting both the bulk fluid and polycrystalline monolayer), with the directors in the plane of the substrate and parallel to the field.

Following the preparation of the uniformly oriented system, samples were removed from the electromagnet, placed in a small convection oven, and heated for different periods of time at different temperatures before cooling again to room temperature to be imaged by STM or polarizing optical microscopy. In most cases, samples were heated above T_{NI} , and in all cases above the melting temperature of the monolayer, T_m . This resulted in the partial (but generally incomplete) loss of order imparted during the first step in sample preparation due to the SME.

The order parameter for the bulk LC was approximated by $S^{\text{bulk}} = \langle (I_0 - I_{45}) / (I_0 + I_{45}) \rangle$, where I_x is the intensity of reflected light measured by a photodiode attached to a polarizing optical microscope with the sample oriented parallel or rotated 45° with respect to one of the crossed polarizers before removing the coverslip, averaged over multiple $\sim 1\ \text{mm}^2$ positions. Note that because the substrate was opaque these measurements had to be performed using reflected light. S^{bulk} provides a useful qualitative measure of order in the cell even though strictly speaking it is not a well constructed order parameter.

To measure orientational order in the 8CB monolayer on HOPG, the coverslip was carefully removed and up to 200 STM images were acquired per sample. Removing the coverslip destroyed order in the supernatant but left the monolayer unaffected.¹⁷ STM is able to image molecules adsorbed to the surface through the supernatant because the bulk fluid is

electrically insulating.¹⁸ Since the orientation of nearby molecular domains was highly correlated, images were taken at multiple macroscopically separated positions. Each image was analyzed to determine the chirality $\chi_i = \pm 1$ ($+1$ = right-handed, -1 = left-handed) and molecular row orientation θ_i^{row} , measured with respect to the original magnetic field axis. Although θ_i^{row} is a prominent and convenient measure of molecular orientation using STM (Figure 1), it is not the axis of highest symmetry in oriented 8CB monolayers, which actually occurs at an angle of $\theta_i = \theta_i^{\text{row}} - \chi_i(56^\circ)$.¹⁹ Using the axis of highest symmetry, the two-dimensional orientational order parameter for the adsorbed monolayer was computed as $S^{\text{ML}} = \langle 2 \cos^2(\theta_i - \bar{\theta}) - 1 \rangle$, where the brackets denote an average over all observations, and $\bar{\theta} = \langle \theta_i \rangle$.

After the first sample preparation step, but before heating, the cells were highly oriented, with initial order parameters $S_0^{\text{ML}} = 0.91$ and $S_0^{\text{bulk}} = 0.76$. When samples were heated during the second preparation step, the order parameters decreased, with the amount of change depending on the heating temperature, time, and cell thickness. In the following, we present results for most of these trends, but we begin with a general observation found to hold for all cells where both STM and polarizing optical microscopy were used: namely, that remnant order in the bulk LC and polycrystalline monolayer closely mirrored one another. This is illustrated by the plot in Figure 1, which collects data from disordering experiments conducted at a variety of heating temperatures ($30\text{--}75^\circ\text{C}$) and times ($10\text{--}120$ min.). Each point represents at least 50 STM observations and $80\text{--}120$ optical measurements from several independently prepared samples. The observed correlation held for cells heated both above and below T_{NI} and provides evidence for strong coupling between surface and bulk molecules.

The effect of heating time and temperature on orientational order in the adsorbed monolayer is shown in Figure 2. The data in Figure 2A were obtained from $20\text{--}40\ \mu\text{m}$ thick cells heated for various times at a fixed temperature of 50°C , which was 9.5°C above T_{NI} , and 16.5°C above T_m . In Figure 2B cells were heated for 20 min. at varying temperatures up to 75°C . Higher temperatures than this could not be reliably probed because impurities began to accumulate on the surface, presumably formed by gradual hydrolysis of 8CB at $T > 75^\circ\text{C}$.²⁰

Figure 2B shows that disordering began when samples were heated to $T \geq T_{\text{NI}}$; below this temperature, S^{ML} was hardly affected by heating. In fact, samples kept at room temperature could be returned to the magnet with a different orientation without altering order in the monolayer, showing the surface dynamics occur only at elevated temperature. A component of order was also observed which could not be erased at the temperature or time scale probed in these experiments. The amount of residual order ($S_\infty \sim 0.1$) was found to be about the same in all experiments, both with and without a magnetic field applied perpendicular to the surface (see below), and reproducible across several different HOPG substrates.

These results indicate a robust memory of the initial orientational state and some mechanism allowing molecules to recover their orientation after the temperature was lowered. For samples heated to $T \gg T_{\text{NI}}$, memory must be associated with molecules at an interface. Since the cells involve two surfaces—a glass coverslip and HOPG substrate—additional experiments were performed to establish which one was responsible for the memory effect. First, cells were constructed by replacing HOPG with a second glass coverslip and subjecting them to the same treatment. Optical microscopy showed these cells displayed almost no memory effect, with essentially all long-range order

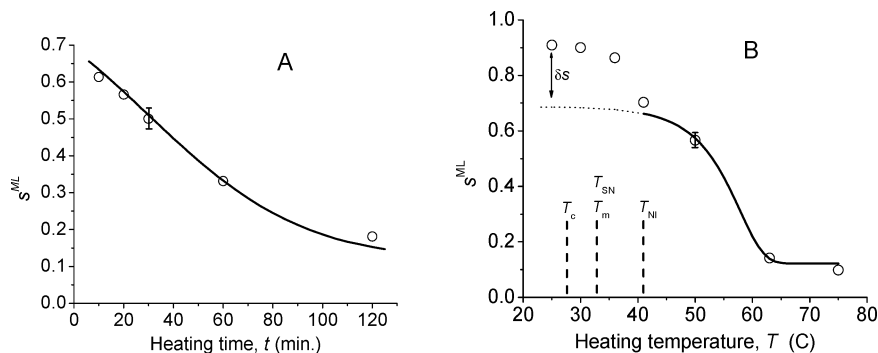


Figure 2. Decay of orientational order in the molecular monolayer adsorbed to graphite as a function of heating time and temperature. Order parameters measured for films heated to (A) 50 °C for varying periods of time, and (B) varying temperatures for 20 min. Data in both figures were simultaneously fit using the model described in the text giving the solid lines. Each point is based on approximately 100 STM images.

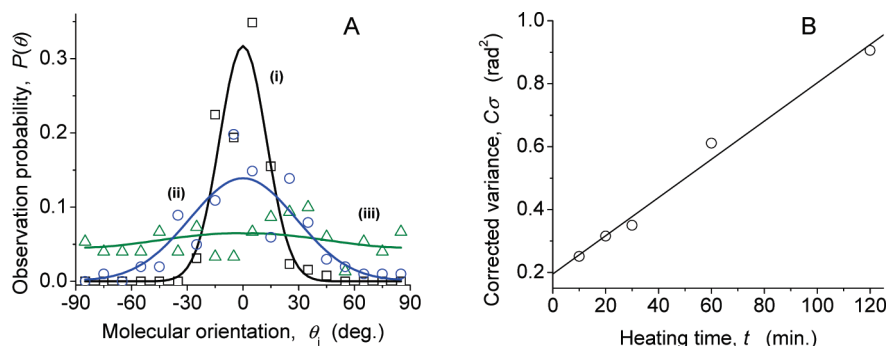


Figure 3. (A) Representative histograms of molecular orientation in the monolayer adsorbed to graphite for samples with three different order parameters: (i) $S^{\text{ML}} = 0.91$, unheated sample, based on 129 STM observations; (ii) $S^{\text{ML}} = 0.61$, $T = 50$ °C, $t = 10$ min, 101 STM observations; and (iii) $S^{\text{ML}} = 0.10$, $T = 75$ °C, $t = 20$ min., 150 STM observations. Solid lines are corrected²² Gaussian functions centered at $\theta_i = 0$ with $\sigma = [-1/2 \ln(S^{\text{ML}})]^{1/2}$. (B) The corrected variance increased linearly with heating time, a hallmark of Brownian rotational kinetics.

destroyed after heating a few degrees Celsius above T_{NI} for short periods of time. Second, very thick (~ 2000 μm) glass/8CB/HOPG cells were constructed, which actually showed a reduced rate of monolayer disordering relative to thin cells subjected to the same thermal sequence, measured by STM. These results indicate that memory is associated with molecules at the HOPG interface, and that the glass interface makes no significant contribution to memory, and possibly produces a small disordering effect.

There are two populations of molecules at the HOPG surface capable of contributing to memory: (i) those adsorbed in deep potential wells at substrate defects, and (ii) those less strongly adsorbed molecules associated with open terrace sites. Previous studies of the SME on indium–tin oxide and polymer surfaces have found large activation barriers for memory erasure—often exceeding the desorption energy^{8,10,13}—and consequently (i) has often been assumed, although no direct measurements have ever been performed to confirm this. As discussed below, we observe a similarly large energy barrier. Setting aside for the moment the question of whether such large barriers are physically reasonable, to gauge the relative contributions of (i) and (ii) we conducted a detailed survey of HOPG substrates by atomic force microscopy to determine the density of defect sites where strong adsorption might occur. Surprisingly, their coverage was found²¹ to be only ~ 0.002 ML, which appears much too low to explain the majority of the memory effect, although perhaps large enough to account for the smaller portion of remnant order S_∞ unaffected by heating. This suggests most memory is retained by molecules associated with open terrace sites, where molecule–substrate interactions are relatively weak.

To better understand the kinetics of the disordering process, Figure 3A presents orientational distributions of surface mol-

ecules for several representative data points from Figure 2. The distributions are approximately Gaussian in shape, with variance σ and a mean molecular orientation $\bar{\theta} = \langle \theta_i \rangle \approx 0$. As shown in Figure 3B, the corrected²² variance of the distributions increased linearly in time as samples were heated. Both properties are hallmarks of Brownian rotational kinetics, where for a collection of two-dimensional rotators the variance is described by $\sigma(t) = 2Dt + \sigma_0$, where σ_0 is the initial variance before heating a sample, t is the heating time, and D is the rotational diffusion coefficient. For a Gaussian distribution centered at $\bar{\theta} = 0$ in two dimensions, one can show that $S^{\text{ML}} = e^{-2\sigma^2}$, where the variance σ is expressed in (radians)². Assuming an activated rotational diffusion model with diffusivity $D = \nu e^{-E_{\text{app}}/kT}$, where ν (radians² s⁻¹) is an attempt frequency, E_{app} is an apparent rotational barrier height, and k is Boltzmann's constant leads to the phenomenological expression:

$$S^{\text{ML}} = S_1 \exp\{-8\nu^2 t^2 e^{-2E_{\text{app}}/kT} - 4\sigma_0 \nu t e^{-E_{\text{app}}/kT}\} + S_\infty \quad (1)$$

where $S_1 = e^{-2\sigma_0^2}$ and S_∞ is the component of residual order not affected by heating.

As shown by the solid lines in Figure 2, for temperatures $T \geq T_{\text{NI}}$ the disordering rate is well described by eq 1 where the constants determined by simultaneously fitting both time- and temperature-dependent data series were $E_{\text{app}} = 130 \pm 20$ kJ mol⁻¹, $\nu = 10^{17 \pm 5}$ rad² s⁻¹, $S_1 = 0.57 \pm 0.05$, and $S_\infty = 0.1 \pm 0.05$. The order parameter given by eq 1 at $t = 0$ is $S_1 + S_\infty = 0.75$, which is less than the initial order parameter measured for unheated cells ($S_0^{\text{ML}} = 0.91$). The difference $\delta S \sim 0.2$, indicated in Figure 2B, may be attributed to removal of the ordering influence of the magnetic field during the second

heating step, which when present enforces uniformity of orientation across an entire sample.

As mentioned above, E_{app} is often found to be very large in studies of the SME. Consistent with this trend, a value several times greater than the activation energy for tumbling rotation in the isotropic phase of 8CB ($29\text{--}41\text{ kJ mol}^{-1}$)²³ was observed, approaching the desorption energy of 8CB from HOPG measured in vacuum ($149 \pm 3\text{ kJ mol}^{-1}$).¹⁴ To understand this result and to reconcile it with the finding that few molecules can be trapped in deep potential wells, let us review the sequence of events occurring during cooling from above T_{NI} . The first phase transition ($40.5\text{ }^{\circ}\text{C}$) involves nucleation of the nematic phase. At this point, the orientation of the nematic director will be influenced by remnant order persisting at the surface through adsorbate populations (i) or (ii). Since no other forces are present to break the azimuthal degeneracy, a modest degree of in-plane anisotropy at the surface can have a pronounced influence on the director orientation of the nematic phase at this stage. Consequently, the bulk nematic can recover much of its original orientation even if remnant order in the surface layer is small, which is not uncommon.²⁴ Ouchi et al. for example found a strong SME on polyimide caused by a surface layer with an order parameter of ~ 0.03 .¹³ Reducing the temperature further, the supernatant enters the smectic-A phase ($33.5\text{ }^{\circ}\text{C}$). For the most part, the smectic-A texture maintained the orientation of the nematic phase from which it formed, as we confirmed by observing samples in the process of cooling using optical microscopy, which showed that orientational order in the supernatant was re-established while in the nematic phase. Finally, at a still lower temperature ($26\text{--}28\text{ }^{\circ}\text{C}$) the monolayer adsorbed to HOPG recrystallizes. The orientation of crystallizing surface molecules is therefore influenced through contact with the oriented supernatant smectic LC via anchoring forces, which produce an elastic torque encouraging coalignment of the bulk and surface directors.^{3,7} Crystallization of the monolayer freezes the dynamics, completing the sequence of bidirectional bulk \leftrightarrow interfacial layer interactions producing the SME.

This picture accounts for the high degree of correlation between S^{ML} and S^{bulk} shown in Figure 1, and why it holds over such a broad range of order parameters. It also explains the anomalously large erasure energies mentioned above: E_{app} overestimates the true rotational diffusion barrier, perhaps substantially so, since it is measured after the system has recovered and cooperativity has amplified a small remnant surface anisotropy. This affects both the present study and previous investigations of the SME.^{6–13}

The principal feature that is new in this interpretation is the bidirectional character of the interaction coupling S^{ML} and S^{bulk} . The interaction has two roles: first to allow remnant order in the surface layer to orient the nematic phase, and second to imprint the orientation of the smectic phase on the crystallizing monolayer. To directly test this, we wish to conduct an experiment in which the interaction has been perturbed in some way and measure the effects on memory. The perturbation should not affect the sequence of phase transitions, alter the amount of remnant order persisting through populations (i) or (ii), or introduce azimuthal anisotropy into the system. One way to do this might be to prepare very thin films, removing the supernatant altogether. If the above picture is correct, the memory effect would be eliminated. However, this experiment is problematic for two reasons. First, it would not be possible to prepare samples in a uniformly oriented initial reference state, since the magnetic field acts primarily on the bulk LC and is not strong enough to significantly affect the monolayer by

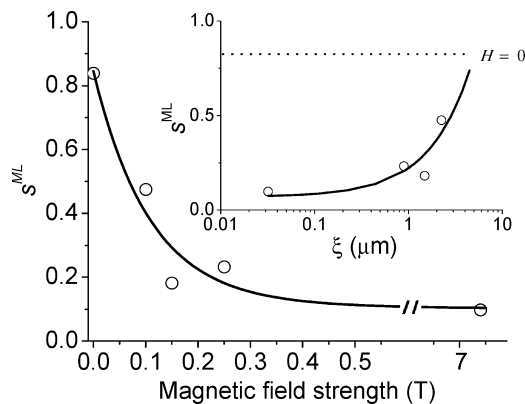


Figure 4. A magnetic field applied perpendicular to the substrate increased the rate of disordering in the 8CB monolayer adsorbed to graphite. Data were taken after heating samples in thick cells at $50\text{ }^{\circ}\text{C}$ for 20 min. Inset shows how the order parameter approaches its unperturbed value ($H = 0$) as the magnetic extrapolation length approaches $\sim 5\text{ }\mu\text{m}$. Solid lines are a guide to the eye.

itself.^{25,26} Second, a monolayer at a graphite/air interface would experience a different chemical environment than one at a graphite/LC interface, potentially shifting transition temperatures and affecting melting and crystallization mechanisms.

An alternative approach that avoids these complications is to apply a magnetic field perpendicular to the substrate during the disordering/reordering steps. A strong enough field will alter the director configuration in the cell by forcing homeotropic alignment in the nematic phase at distances from the substrate exceeding the magnetic extrapolation length, $\xi \approx H^{-1}\sqrt{K/\Delta\chi}$, where H is the field strength, K is an elastic constant, and $\Delta\chi$ is the magnetic susceptibility anisotropy.²⁷ As the strength of the field increases, ξ decreases and the interfacial layer–supernatant LC interaction is more strongly perturbed; in the limit $\xi \rightarrow 0$ the bulk director becomes uniformly homeotropic and the azimuthal component of the interaction is entirely eliminated by symmetry. Although elastic and anchoring forces prevent this limit from being reached, if the cooperative interactions extend farther than ξ into the bulk, application of the field should result in a decrease of S^{ML} with increasing field strength. Furthermore, by measuring the dependence of S^{ML} on ξ (or more precisely, on H) the minimum effective thickness of the supernatant layer needed for the memory effect can also be established.

To perform this experiment, cells thicker than $2000\text{ }\mu\text{m}$ were used to approximate the limiting case of a graphite–8CB interface in contact with a semi-infinite 8CB fluid. This shifted the Fredericks transition to a critical field threshold much lower than the smallest field studied, thereby providing a smooth and continuous evolution of the director profile as a function of magnetic field strength.²⁸ Permanent magnetic rods were used to produce fields up to 0.25 T , and for the highest field strength (7.4 T) samples were placed in a superconducting magnet equipped with a custom sample heater. Note that fields with the strength used here have no appreciable effect on molecules in the surface layer^{25,26} or on the bulk transition temperatures,²⁹ and (near the center of the sample) the field was nearly vertical.

The results of these experiments are shown in Figure 4, where samples were heated to $50\text{ }^{\circ}\text{C}$ for 20 min. Application of an increasingly strong field accelerated the apparent rate of orientational disordering. For the largest field, S^{ML} was reduced by nearly 90% relative to the no-field case, leaving only the component of order S_{∞} previously found to be unaffected by heating. The inset of Figure 4 shows how S^{ML} depends on ξ ,

where the values K and $\Delta\chi$ used to compute ξ are those for nematic 8CB near the monolayer crystallization temperature.³⁰ S^{ML} begins to approach the value of an unperturbed sample at roughly $\xi \sim 5 \mu\text{m}$, indicating the interactions are localized to the near-surface region.

Conclusions

In summary, orientational memory in interfacial LC films was studied by preparing cells in a uniformly oriented initial reference state and separately measuring bulk and surface order parameters as systems were thermally disordered. Strong memory was observed despite relatively weak molecule–surface interactions of the kind previously thought to be responsible for this effect. Although memory erasure appeared to follow Brownian-like kinetics, the underlying events actually entail a series of stepwise disordering and reordering transitions, inflating the apparent memory erasure activation energy. Cooperative interactions between surface and bulk molecules were found to play an important role in the memory effect, leading to the recovery of long-range order that neither layer alone retained. When cooperativity was perturbed using a magnetic field, orientational memory in the surface layer almost disappeared. The findings provide a new interpretation of the origins of orientational memory in liquid crystal films and underscore the potentially important role of cooperativity in bulk \leftrightarrow interfacial liquid crystal interactions.

Acknowledgment. This work was supported by the National Science Foundation under CHE-0518682 and DMR-0705908. The authors thank C. Reinhart, A. Brackley, and B. Edwards for their contributions and B. L. Johnson for insights into the theoretical analysis.

Supporting Information Available: Calculation of the surface order parameter, S^{ML} . This material is available free of charge via the Internet at <http://pubs.acs.org>.

References and Notes

- (1) Zhuang, X.; Marrucci, L.; Shen, Y. R. *Phys. Rev. Lett.* **1994**, *73*, 1513.
- (2) Qian, T.; Zhuang, X.; Shen, Y. R. *Phys. Rev. E* **1999**, *59*, 1873.
- (3) Mougous, J. D.; Brackley, A. J.; Foland, K.; Baker, R. T.; Patrick, D. L. *Phys. Rev. Lett.* **2000**, *84*, 2742.
- (4) Jérôme, B. *Rep. Prog. Phys.* **1991**, *54*, 391.
- (5) (a) Zwicky, F. *Phys. Rev.* **1933**, *43*, 270. (b) Haken, H. *Rev. Mod. Phys.* **1975**, *47*, 67.
- (6) Friedel, G. *Ann. Phys. (Paris)* **1922**, *18*, 273.
- (7) Clark, N. A. *Phys. Rev. Lett.* **1985**, *55*, 292.
- (8) Nych, A. B.; Reznikov, D. Y.; Boiko, O. P.; Nazarenko, V. G.; Pergemshchik, V. M.; Bos, P. *EPL* **2008**, *81*, 16001.
- (9) Akiyama, H.; Yoshida, N.; Nishikawa, M.; Kobayashi, S.; Iimura, Y. *Jpn. J. Appl. Phys.* **1997**, *36*, L1204.
- (10) Petrov, M. P.; Tsonev, L. V. *Liq. Cryst.* **1996**, *21*, 543.
- (11) (a) Tsonev, L. V.; Petrov, M. P.; Barbero, G. *Liq. Cryst.* **1998**, *24*, 853. (b) Tsonev, L.; Petrov, M.; Barbero, G. *Liq. Cryst.* **2000**, *27*, 825.
- (12) Jérôme, B.; Schuddeboom, P. C.; Meister, R. *Europhys. Lett.* **2002**, *57*, 389.
- (13) Ouchi, Y.; Feller, M. B.; Moses, T.; Shen, Y. R. *Phys. Rev. Lett.* **1992**, *68*, 3040.
- (14) Patrick, D. L.; Cee, V. J.; Beebe, T. P., Jr. *J. Phys. Chem.* **1996**, *100*, 8478. 1996.
- (15) Rivera Hernandez, M.; Miles, M. J. *Probe Microsc.* **2000**, *2*, 45.
- (16) Lacaze, E.; Alba, M.; Barré, J.; Braslau, A.; Golmann, M.; Serreau, J. *Physica B* **1998**, *248*, 246.
- (17) Once the monolayer crystallized, it was remarkably robust toward perturbations of the supernatant fluid. We have observed, for example, that after crystallization most of the bulk LC can be removed by scraping it off with a soft rubber blade without causing any measureable change in orientational order of the monolayer.
- (18) Foster, J. S.; Frommer, J. E. *Nature* **1988**, *333*, 542.
- (19) Please refer to Supporting Information.
- (20) Stevens, F.; Patrick, D. L.; Cee, V. J.; Purnell, T. J.; Cook, T.; Beebe, T. P., Jr. *Langmuir* **1998**, *14*, 2396.
- (21) Using AFM the step density was found to average $1 \mu\text{m}$ of step edge per $1 \mu\text{m}^2$ of surface area, a figure including both single and multi-atom steps. Assuming each adsorbed molecule occupied 1 nm^2 , step edges accounted for $\sim 0.2\%$ of all adsorption sites. To count atomic-scale defects at open terrace sites they were first enlarged by oxidizing HOPG in air at $\sim 600^\circ\text{C}$, causing the formation of large circular etch pits easily observed by AFM. [Patrick, D. L.; Cee, V. J.; Beebe, T. P., Jr. *Science* **1994**, *265*, 231. Using this procedure 1 point defect per $4 \mu\text{m}^2$ of surface area was found by AFM, giving a coverage of $\sim 2 \times 10^{-5} \%$. 8CB monolayers on graphite contain few impurities because the compound forms a densely-packed film that displaces most other adsorbates. We estimate their surface coverage based on over 2400 STM images acquired in the course of this study to be $\sim 0.1\%$ at room temperature.
- (22) In the experiments, domain orientation was always measured as the acute angle $-\pi/2 \leq \theta \leq \pi/2$, because domains whose orientations differed by multiples of π were indistinguishable. Therefore, the measured variance was always less than the variance of a true Gaussian distribution, where angles outside this range are possible. To correct for this, the measured variance for each sample was multiplied by a correction factor $C(S^{\text{ML}}) = \sigma_{\text{true}}/\sigma_{\text{app}}$, where σ_{true} is the actual variance of a Gaussian distribution with an order parameter S^{ML} and σ_{app} is the apparent variance that would be measured if all angles outside the range $-\pi/2 \leq \theta \leq \pi/2$ were transformed into this range.
- (23) (a) Bose, T. K.; Chahine, R.; Merabet, M.; Thoen, J. *J. Phys. (Fr.)* **1977**, *45*, 1465. (b) Arcioni, A.; Bacchiocchi, C.; Grossi, L.; Nicolini, A.; Zannoni, C. *J. Phys. Chem. B* **2002**, *106*, 9245. (c) Schonhals, A.; Zubowa, H. L.; Fricke, R.; Frunza, S.; Frunza, L.; Moldovan, R. *Cryst. Res. Technol.* **1999**, *34*, 339.
- (24) Xuan, L.; Tohyama, T.; Miyashita, T.; Uchida, T. *J. Appl. Phys.* **2004**, *96*, 1953.
- (25) Barmantlo, M.; Hollering, R. W. J.; Wierenga, H. A.; van Hasselt, C. W. Rasing, Th. *Physica B* **1995**, *204*, 38.
- (26) Boamfa, M. I.; Kim, M. W.; Maan, J. C. Rasing, Th. *Nature* **2003**, *421*, 149.
- (27) de Gennes, P. G.; Prost, J. *The Physics of Liquid Crystals*; Clarendon Press: Oxford, UK, 1993.
- (28) Sonin, A. A. *The Surface Physics of Liquid Crystals*; Gordon and Breach: Luxembourg, 1995.
- (29) Rosenblatt, C. *Phys. Rev. A* **1981**, *24*, 2236.
- (30) $\Delta\chi = 1 \times 10^{-7}$ (cgs units) [Sherrel, P. L.; Crellin, D. A. *J. Phys. Colloq. C3, Suppl. 4* **1979**, *40*, C3-211], $K = 5 \times 10^{-7}$ dyn [Faetti, S.; Palleschi, V. *Liq. Cryst.* **1987**, *2*, 261].

JP909218G